17th World Conference on Earthquake Engineering, 17WCEE
Sendai, Japan - September 13th to 18th 2020

LARGE-SCALE TESTING OF A CONCENTRICALLY BRACED FRAME WITH REPLACEABLE BRACE MODULES

V. Mohsenzadeh[(1)], L. Wiebe[(2)]

[(1)] *PhD Candidate, Department of Civil Engineering, McMaster University, mohsenzv@mcmaster.ca*
[(2)] *Associate Professor, Department of Civil Engineering, McMaster University, wiebel@mcmaster.ca*

Abstract

Special concentrically braced frames are one of the most common seismic force resisting systems in regions of high seismicity because of their high strength and stiffness. This system relies on tensile yielding and compression buckling of diagonal braces to dissipate energy. In current practice, a gusset plate is used to join the brace to the frame elements. Following a capacity design procedure and using geometrical limits to achieve the required out-of-plane deformation capacity may result in large and uneconomical gusset plates. Moreover, recent experiments have shown that toe weld fractures at the gusset plate, partly due to the opening and closing of the beam-to-column joint, can limit the drift capacity of the system. A more seismically resilient connection has recently been developed based on the concept of a Replaceable Brace Module (RBM). This connection does not require field welding as it can be bolted into place, and it is intended to make the frame easily repairable by confining all damage to the RBM. Previous testing of individual modules has shown that the proposed connection holds promise as an alternative for concentrically braced frames. However, there has not previously been any experimental study of this connection at the system level. This paper discusses the first large-scale testing of a single-storey and single-bay concentrically braced frame with RBM and a shear tab beam-column connection, performed at McMaster University. This experimental study simulates the interaction of all the braced frame components including bracing members, the proposed connection, beam-to-column connection, beam, and column. The experimental program consists of two phases. In the first phase, the frame is subjected to quasi-static cyclic loading up to fracture of one brace. In the second phase, the damaged RBMs are replaced with the new RBMs, and the behaviour of the frame is investigated under the same loading protocol. This paper presents preliminary results from the tests as a step towards making the proposed RBM available for use by design engineers in practice.

Keywords: concentrically braced frames; replaceable brace modules; beam-column connection

1. Introduction

Current seismic design procedures are able to control effectively the casualties caused by earthquakes. However, the economic loss and social influence are still enormous. While damage to buildings and infrastructure causes direct economic loss due to an earthquake, an earthquake also results in indirect loss because of temporary suspension or reduced use of structures. If structures could regain their functionality more quickly after the earthquake, the indirect loss would be reduced. For that reason, the study of earthquake resilient structures has become one of the new promising directions in the earthquake engineering. An earthquake resilient structure is ome that can rapidly restore its structural functionality after a severe earthquake without significant repair [1]. One way of making more earthquake resilient structures is by using replaceable structural components, where the damage due to the earthquake will concentrate in these components that can be easily replaced after an earthquake. This allows the strucure to be more easily reparable after an earthquake.

With this in mind, the concentrically braced frame (CBF) with replaceable brace modules (RBMs) is a system with an alternative connection for connecting the brace to the beam as shown in Fig. 1. Instead of requiring field welding, bolts are used to connect the brace to the beam, which improves the constructability of CBFs by providing easier and more accurate installation. The bolted connection allows all the damage to be confined to an easily replaceable assembly and results in fast repair in the event of damage. The brace also buckles in the in-plane direction, reducing the potential for damage to partitions and cladding.

An experimental study at the component level was conducted to ensure that a brace with the new alternative connection would be able to provide the desired benefits, and that its seismic performance would be comparable to braces with conventional gusset plate connections [2]. Eight 2:3 scale RBMs with hollow structural sections were tested and the results showed that braces with the new alternative connection will perform satisfactorily in terms of intended hinge location, failure development, drift range before brace fracture, and cumulative energy dissipation. However, braced frame behaviour is highly system dependent, and in order to predict the performance accurately, the contribution of frame elements must also be considered [3]. Therefore, large-scale system-level experimental testing is required to consider the contribution of frame element in a CBF with RBMs.

This paper presents 70%-scale testing of a single-storey and single-bay concentrically braced frame with RBMs and shear tab beam-column connections in the Applied Dynamics Laboratory at McMaster University. The objectives of this experimental study include evaluating the performance of CBF system with RBMs, investigating the seismic performance of the shear tab connecion in a CBF with RBMs, and examining brace replaceability and the CBF seismic behaviour with replaced RBMs.

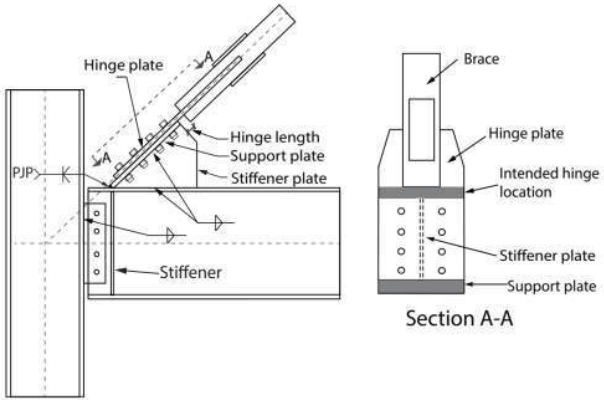

Fig. 1 – Replaceable brace module connection details

2. Laboratory Program and Setup

2.1 Test Setup

Fig. 2 shows the test frames, which represented a 70%-scale model of a second floor braced bay for a reference structure in Vancouver, British Columbia which was designed based on the Canadian code [4]. The structure was designed according to the provisions of CSA S16-14 [5] for moderately ductile concentrically braced frames (MD-CBFs), which have similar design requirements to special concentrically braced frames (SCBFs) in AISC 341 [6] and can be used in regions of high seismicity. The test specimen is intended to be typical of what would be found in a lower storey of a low- to mid-rise structure.

The setup was designed to capture the frame contribution in an actual building as accurately as possible. For that reason, boundary conditions should be considered in a way that the moment and shear demands in frame members are simulated correctly in the experimental study. To find the appropriate boundary conditions, nonlinear static analysis of a model of the reference building shown in Figure 2(a) was performed in SAP2000 [7] following ASCE-SEI 41-17 [8] recommendations, applying lateral load in a way that imposed a large inter-storey drift at the level of interest. The second storey was chosen because one of the main objectives of this study was testing the performance of the proposed beam-column connection where the RBM connects to the beam. Then the moments on columns, and rotation demand on beam-column connections were investigated and boundary conditions were designed to simulate the actual behaviour with reasonable accuracy. Two horizontal struts were designed to simulate the stiffness of the braces below the

level of interest, and were connected to strong brackets mounted on the lab floor. For the bottoms of the columns, pinned connections were placed at the approximate location of the point of inflection in the lower storey that was found during the reference analysis. At the top, the columns were extended and connected to a rigid-strong beam using a rigid connection, again based on the column bending moment diagram that had been found in the reference analysis. Gravity load-induced axial load on the columns could not be simulated within the laboratory constraints of this study.

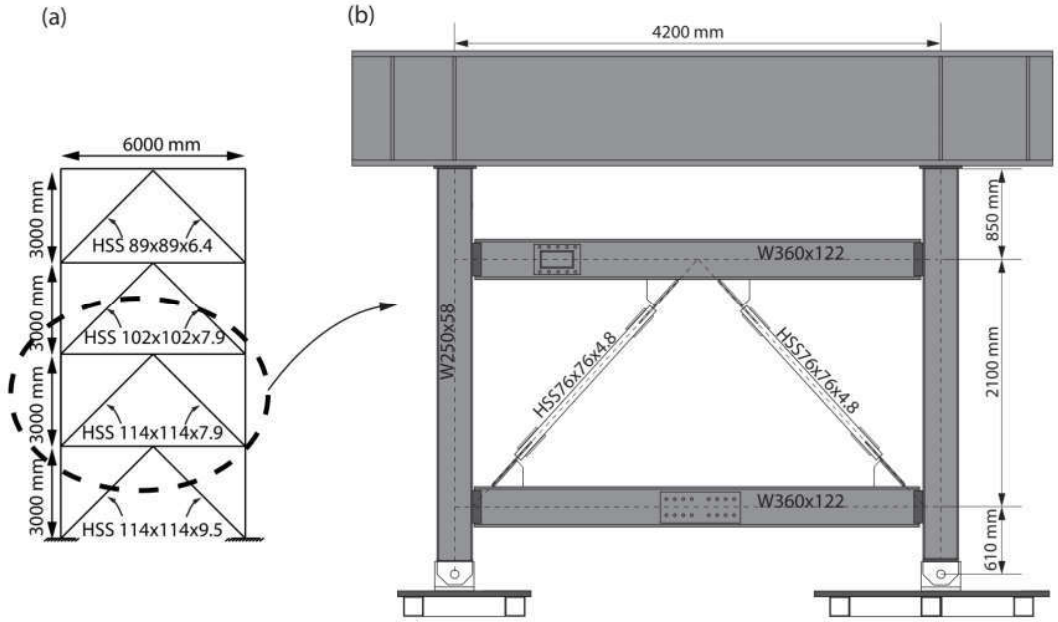

Fig. 2 – (a) Reference considered braced bay, (b) prototype specimen

Fig. 3(a) and (b) show the AutoCAD drawing and photo of the test setup, respectively. The test setup contained a reaction frame, a loading frame, and the specimen. The horizontal displacement was applied to the loading frame beams using a 1000 kN capacity 500 mm stroke actuator under displacement control. The loading beams were connected to the loading frame columns by plates with slotted holes using a detail proposed by Eatherton and Hajjar [9] to resist the axial forces and accommodate the rotation of the beam relative to the loading frame columns under large drifts. In order to transfer the load from the loading frame beams to the upper beam of the specimen, two slip-critical bolted connections were used. The loading frame columns were attached to the strong platform through pin connections to minimize any unintended contribution to the lateral resistance. Out-of-plane support was provided to the rigid-strong beam using two 75 mm diameter 250 mm stroke implement cylinders that resisted out-of-plane displacements, based on laser displacement transducers as the input for the control system.

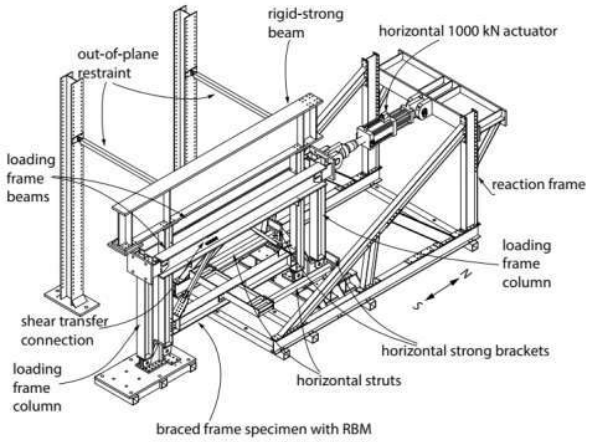

(a)

(b)

Fig. 3 – Layout of test setup (a) drawing, (b) as-built photo

2.2 Frame Design

In the specimen that was tested, wide-flange beams were connected to the wide-flange columns through shear tab connections while square hollow structural sections (HSS) were used for braces. All braces were G40.21 350W Class C members [10]. The beams and columns were ASTM A992 [11] sections with yield and ultimate strengths of $F_y = 360MPa$ and $F_u = 488MPa$, respectively, according to the mill certificates.

The RBM connections were designed to resist the overstrength capacity of the brace. Although the bolts were not designed for a calculated slip load, they were pretensioned up to 70% of their ultimate tensile capacity using a torque wrench. The hinge plates (see Fig. 1) were also designed such that all limit state resistances including gross yield, net section fracture, and the block shear of the hinge plate were stronger than the overstrength capacity of the brace. The support plate and the stiffener plate had the same thickness as the associated hinge plate. The hinge length, defined as the distance between the end of the support plate and end of the brace (see Fig. 1) was twice hinge plate thickness [12].

Table 1 summarizes the key parameters of the braces, including the expected yield strength ($R_y F_y$) from CSA S16-14 [5], local slenderness (b_{el}/t), slenderness ratio (KL/r), and overstrength capacity of the brace in tension ($T_u = R_y F_y A_g$) and in compression ($C_u = 1.2C_r$) and. Hinge plates can provide flexural rotational restraints at the end of the brace, resulting in a smaller effective length (KL) of the brace. To account for that, a theoretical effective buckling length factor was defined based on a three-hinge mechanism using Eq. (1) [13].

$$K = \frac{1}{1 + (\frac{M_{ph}}{M_{pb}})} \tag{1}$$

where M_{ph} is the plastic moment capacity of the hinge plate, and M_{pb} is the plastic moment capacity of the brace. The slip load of the connection that is shown in Table 1 was calculated with the formula from CSA S16 [5], using a resistance factor of one and assuming clean mill scale conditions, as were present in the tests.

Table 1 – Brace details

Designaion	R_yF_y (MPa)	F_u (MPa)	L (mm)	b_{el}/t	M_{ph} (kN.m)	M_{pb} (kN.m)	K	KL/r	T_u (kN)	C_u (kN)	Slip load (kN)
HSS 76x76x4.8	450	514	1775	11.90	3.70	15.48	0.81	49.3	590	536	299

2.3 Shear Tab Connection Details

Fig. 4 shows the single shear tab connection (STC) detail that was tested in this experimental study. The shear tab was welded to the column in the shop and bolted to the beam in the lab. A single shear tab connection was chosen for ease of fabrication and erection. Short slotted holes were designed for the shear tab plate in order to permit larger connection rotations while delaying damage. To prevent beam flange bending and web buckling, stiffeners were provided at the location of the support plate. The beam-column connection was designed to carry both vertical and horizontal forces, but no moment. Although the eccentricity of this connection load on the column produces a moment, it does not increase the peak force demand on columns because the maximum axial load-moment interaction happens at larger inter-storey drifts where the moment contribution is maximized due to non-uniform storey drifts, whereas the braces have buckled and place relatively little flexural demand on columns [14].

2.4 Loading Protocol and Instrumentation

The testing occurred in two phases. In the first phase, the loading protocol described below was applied until fracture of one RBM. In the second phase, the damaged RBMs were replaced, and the same loading protocol was then reapplied.

The loading was applied cyclically and quasi-statically following the ATC-24 testing protocol [15]. Fig. 5 shows the typical deformation history that was applied in increments of the predicted inter-storey drift of the frame at the onset of the first buckling (D_y). If no brace fractured by the end of this protocol, the load protocol was extended with cycles at $+1D_y$ relative to previous displacement until failure. In the second phase of testing the specimen, after both braces had fractured, in order to investigate the post-fracture stiffness and resistance of the braced frame with RBMs, the loading was continued using large inelastic cycles.

The applied load was measured by a load cell connected to the actuator. String potentiometers were used to measure inter-storey drift, axial deformation and in-plane deflection of braces. Beam-column connection rotations were measured using linear variable displacement transducers (LVDT). Strain gauges were used on the braces, columns and beams to establish the forces in elements.

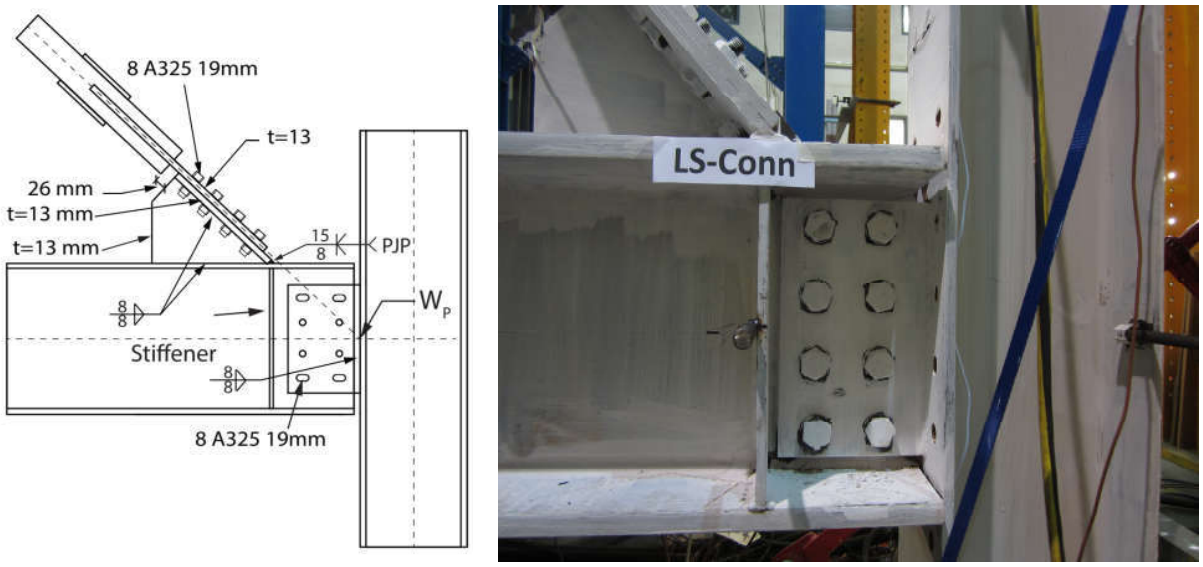

(a) (b)

Fig. 4 – Shear tab connection (STC) (a) drawing, (b) as-built photo

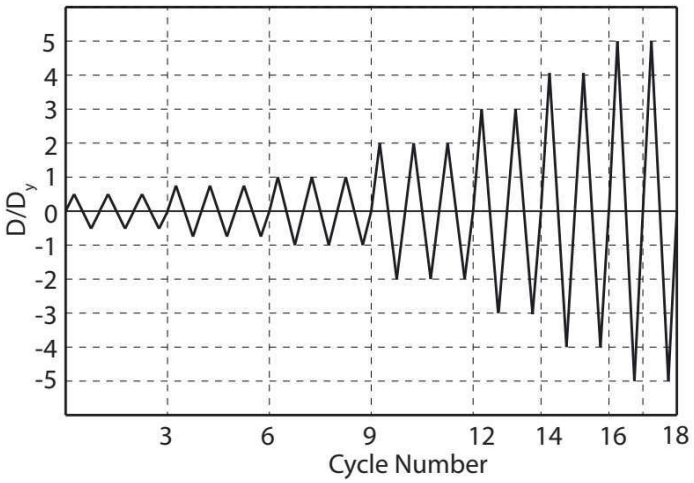

Fig. 5 – Load protocol

3. Overall Frame Response

In this study, the inter-storey drift range, defined as the sum of the maximum drifts of both compression and tension excursions, is the main parameter that is used for assessing the performance. The hysteresis of the base shear vs inter-storey drift ratio is plotted in Fig. 6, where Fig. 6(a) shows the results during the first phase, and Fig. 6(b) shows the response of the system during the second phase (i.e. after replacing the damaged braces). A positive displacement indicates that the actuator is pushing the frame. The shear force is shown after dividing by $2C_r \cos\theta$ of the braces, where θ is the brace angle to the horizontal. In designing

CBF systems, a design engineer will select the brace sections such that the design horizontal shear force at each level will be smaller than $2C_r \cos\theta$ of the braces. For that reason, $2C_r \cos\theta$ is a good estimation of the design shear resistance of the braced frame.

In the first phase, in-plane buckling of the braces was visually observed at about ±0.55% drift (see Fig. 7(a)), and the hinge plates began to yield in flexural due to brace buckling deformation at the same storey drift. Local cupping of the braces due to high compressive axial and bending strains was noted at about 1.35% (Fig. 7(b)). The south brace fractured first at the middle of the brace at 1.63% drift when it was in tension (see Fig. 7(c)), and then the frame lost 25% of its design shear resistance. The frame was then unloaded to allow replacement of the RBMs for the second phase. During the first phase, the maximum drift range of the frame prior to south brace fracture was 3.6%, and the maximum lateral resistance was -760 kN and +675 kN in the north and south directions, respectively.

Figs. 7(d) and (e) show that the hinge plate yielded in flexure in slightly different regions at each end of the brace, depending on the direction of buckling relative to the connection. This occurred because the support plates are located at different sides of the brace at the top and bottom. Even with this slight asymmetry in hinge plate yielding, significant yielding was observed without any unintended damage. The columns and beams did not yield during this phase of testing.

After unloading at the end of the first phase, the residual drift was 0.6%, but the RBMs were removed without difficulty. After straightening the frame, the new RBMs were installed, and the second phase of testing was conducted. Fig. 6(b) shows that the resistance of the frame during the second phase was within 9% of what was observed during the first phase, with maximum storey shears before brace fracture of -830 kN and +648 kN and a drift range of 3.7% before fracture of both braces. In-plane buckling and local cupping initiated during the same loading cycles in the second phase as in the first, although the north brace buckled downwards instead of upwards. A significant loss of 66% of the frame design shear resistance was detected after fracture of the second brace.

After both braces fractured, loading was continued up to ±3.35% (drift range of 6.7%). At these large drifts, the frame provided lateral resistance of as much as 80% of $2C_r \cos\theta$. This resistance was within 2% of the expected limit calculated based on both columns reaching their plastic moment capacity, M_p, at the centres of the top and bottom beams. Yielding of the columns in flexure was first observed at the tops of the columns around 2.80% inter-storey drift. No crack was observed in any welds, and no local inelastic deformation was recognized in the beams in both phases.

Table 2 summarizes the key parameters of the behaviour. The drift range that was observed for the specimen in both phases of testing is comparable to the expected values for SCBFs with more conventional gusset plate connections (e.g. [16]). As shown in Table 2, the initial elastic stiffness of the frame in the second phase was within 8% of its value in the first phase. After both braces fractured, a 90% decrease was measured in the stiffness.

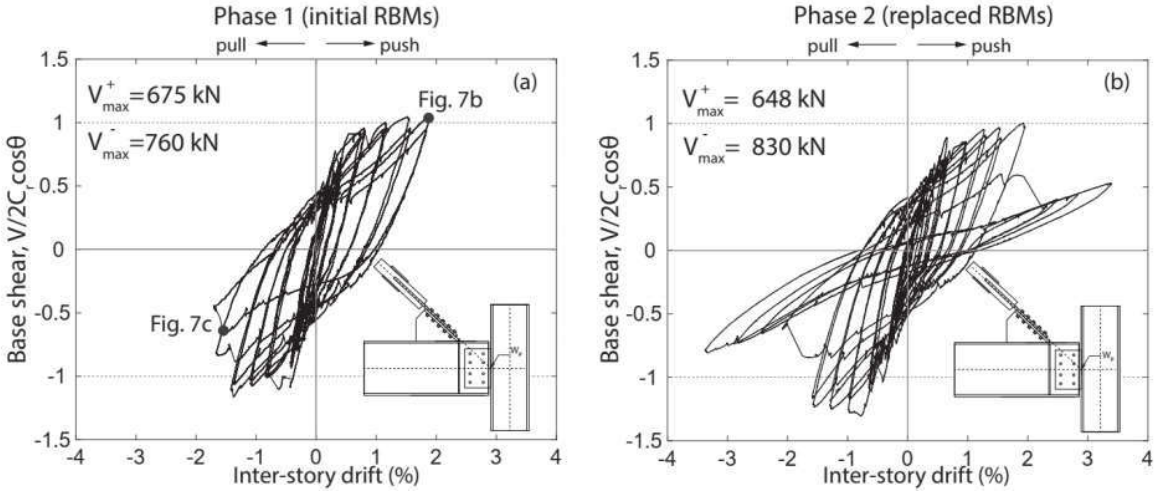

Fig. 6 – Cyclic static results for (a) first phase of testing, (b) second phase of testing

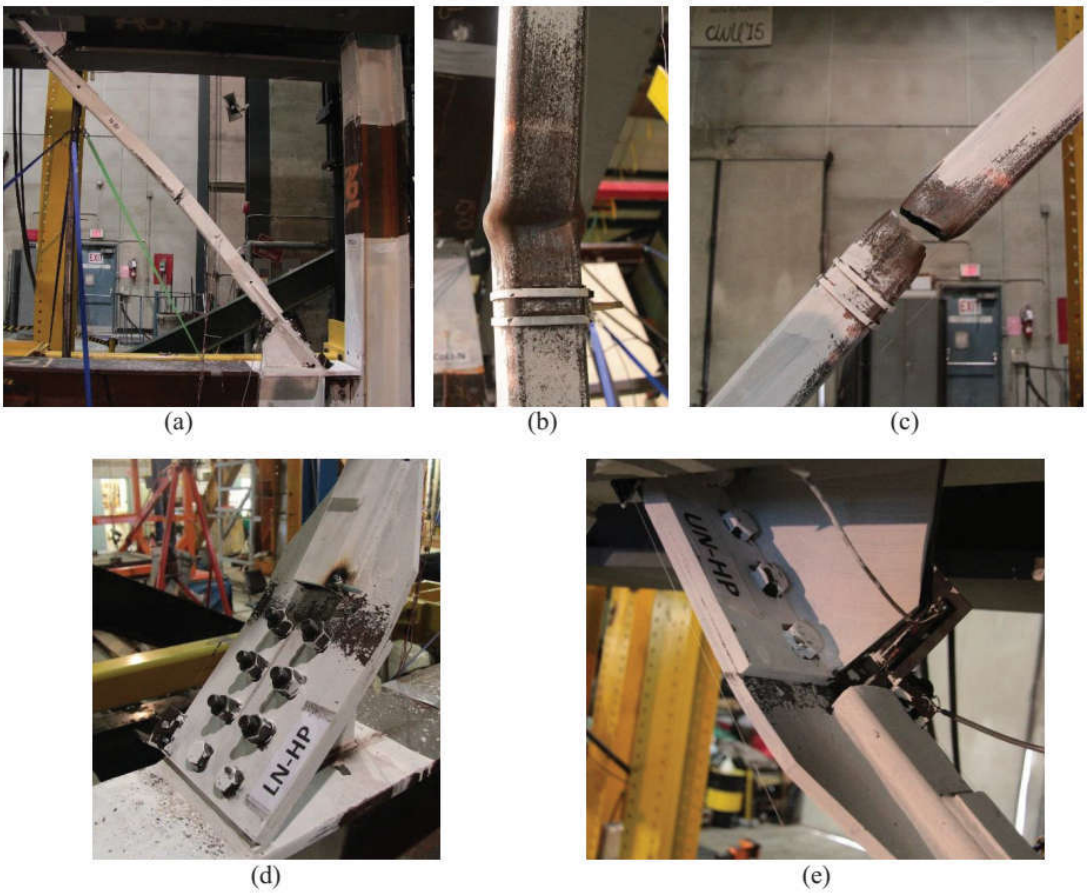

Fig. 7 – Photos of observed behaviour (a) initial north brace in-plane buckling, (b) south brace local cupping, (c) south brace fracture, (d) north brace bottom hinge plate, (e) north brace top hinge plate

Table 2 – Specimen behaviour summary

Parameter	Specimen with STC	
Phase number	Phase 1 Initial RBMs	Phase 2 Replaced RBMs
Failure mode	Brace fracture	Brace fracture
Predicted base shear at brace buckling, V_{bb} (kN)	644	644
Maximum base shear V / V_{bb}	-1.18/+1.05	-1.28/+1.01
Drift at 1st brace fracture (%)	-1.63 (south brace)	-1.75 (south brace)
Drift at 2nd brace fracture (%)	N/A	-1.94 (north brace)
Maximum drift range (%)	3.6	3.7
Residual drift (%)	0.60	N/A
Elastic stiffness (kN/%)	1140	1325
Stiffness after braces fracture (kN/%)	N/A	147

4. Beam-Column Connection

The behaviour of the shear tab connection was investigated using the connection rotation versus inter-storey drift curves shown in Fig. 8. This Figure shows results from the second phase of testing, where higher rotation demand was applied to the connection. Fig. 8(a) shows that the connection sustained rotations of more than 0.032 rad without any loss of rotational capability or local damage in the beam flanges and web. The slightly slotted bolt holes in the shear tab appeared to improve the performance of the connection in terms of rotation capacity and ductility. Fig. 8(b) shows the lower south connection at its largest rotation. The lower acceptable rotation limit of 0.025 rad for a simple beam-column connection rotation capacity where a brace connects to the frame elements, suggested by Seismic Provisions for Structural Steel Buildings [6], was satisfied for this specimen.

5. Brace End Connection Behaviour

The hinge plate rotation within the brace end connections was measured using LVDTs. The results showed that the maximum rotation varied between 0.12 to 0.15 rad, which is about 75% of the values reported for regular gusset plates [16]. Because the hinge plate width was limited to be no more than the beam width, so as to avoid interfering with the surrounding elements, the hinge plate was thicker than a typical gusset plate would have been. As such, considering that hinge plates are likely to provide higher rotational stiffness and subsequently smaller rotations at the end of the brace, use of Eq. (1) is especially important when calculating the effective length.

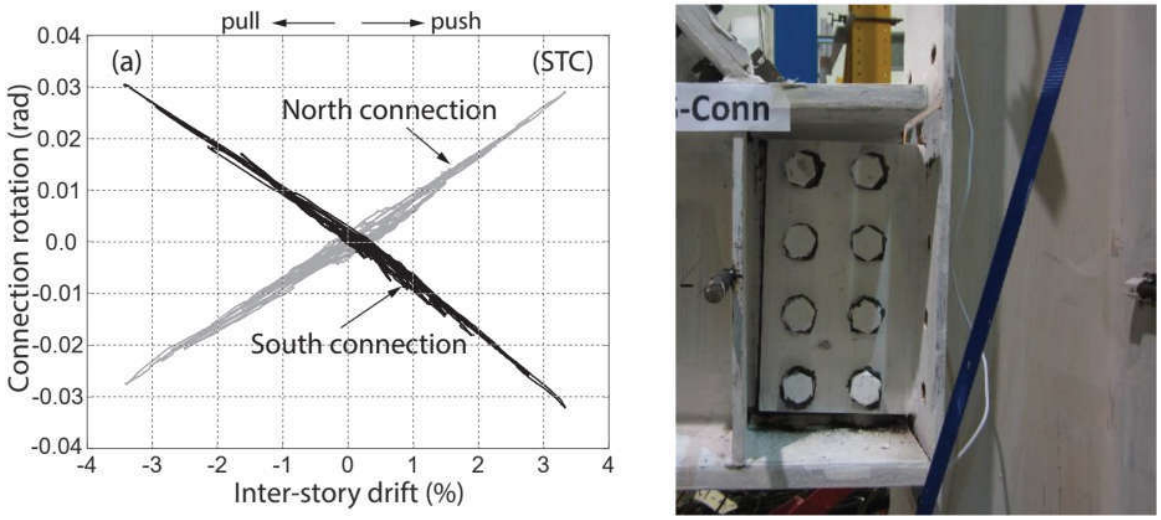

(a) (b)

Fig. 8 – Shear tab connection (STC) performance (a) connection rotation vs inter-storey drift, (b) connection at 0.032 rad rotation

5. Conclusions

The experimental study program presented here was the first large-scale testing of a single-storey and single-bay concentrically braced frame with replaceable brace modules. This study focused on the overall system-level performance of the frame, behaviour of the shear tab beam-column connection, and hinge plate behaviour. The study was conducted in two phases, first with initial brace modules and then with replaced brace modules to examine the brace module replaceability and the behaviour of the frame with replaced brace modules. The study indicated that:

- In both phases, braces buckled in the in-plane direction and damage was confined to the replaceable brace modules.
- In both phases, the specimen sustained multiple inelastic cycles, and reached the nominal design shear resistance.
- Hinges formed in the intended locations in the hinge plates, and no connection failure was observed.
- Despite the residual drift at the end of the first phase, the brace modules were removed easily and new brace modules were installed after straightening the frame.
- The results demonstrated that the shear tab connection with replaceable brace modules performed well and the frame performance was comparable to what would be expected with more traditional connection approaches.

The testing showed the viability of the proposed new approach for detailing concentrically braced frames to facilitate both initial construction and rapid repair after an earthquake.

6. Acknowledgements

Funding for this project has been provided by the Canadian Institute of Steel Construction (CISC) and the National Sciences and Engineering Research Council (NSERC). The wide flange sections were donated by Salit Steel and the HSS sections were donated by Atlas Tube. Fabrication services were provided by Walters Inc. The authors gratefully acknowledge their support.

7. References

[1] Liu Q, Jiang H (2017): Experimental study on a new type of earthquake resilient shear wall. *Earthquake Engineering & Structural Dynamics*, 46 (14), 2479–97.

[2] Stevens D, Wiebe L (2019): Experimental testing of a replaceable brace module for seismically designed concentrically braced steel frames. *Journal of Structural Engineering*, 145. 04019012

[3] Uriz P, Mahin SA (2008): Toward earthquake-resistant design of concentrically braced steel-frame structures. *Technical Report PEER 2008/08*, Pacific Earthquake Engineering Research, Berkeley, USA.

[4] NRC (2015): National building code of Canada 2015. NBCC-15. Ottawa, Canada: NRCC

[5] CSA (2014): Limit state design of steel structures. CAN/CSA S16-14. Canadian Standard Association, Toronto, Canada: CSA.

[6] AISC (2016): Seismic provisions for structural steel buildings. ANSI/AISC 341, Chicago, USA: AISC.

[7] Computers and Structures Inc. (2016): Structural Analysis Program, SAP-2000NL Version 16.0.0: *Integrated Finite Element Analysis and Design of Structures*. Berkeley, USA.

[8] ASCE (2017): Seismic rehabilitation of existing buildings. ASCE/SEI 41-17, Chicago, USA: AISC.

[9] Eatherton MR, Hajjar JF (2010): Large-scale cyclic and hybrid simulation testing and development of a controlled rocking steel building system with replaceable fuses. *Report No. NSEL-025,* Newmark Structural Engineering Laboratory, Urbana, USA.

[10] CSA (2013): General requirements for rolled or welded structural quality steel/structural quality steel. G40.20-13/G40.21-13, Mississauga, Canada: CSA.

[11] ASTM-A992/A992M-11 (2015): Standard specification for structural steel shapes. ASTM International. West Conshohocken, USA.

[12] Astaneh-Asl A, Goel S, Hanson R (1985): Cyclic out-of-plane buckling of double-angle bracing. *Journal of Structural Engineering*. 111 (5), 1135-1153.

[13] Takeuchi T, Matsui R (2015): Cumulative deformation of capacity of braces under various cyclic loading histories. *Journal of Structural Engineering*. 141 (7), 0401417.

[14] Mohsenzadeh V, Wiebe L (2019): Seismic design of columns in concentrically braced frames with replaceable brace modules. *12th Canadian Conference on Earthquake Engineering*, Quebec, Canada.

[15] ATC (1992): Guidelines for cyclic seismic testing of components of steel structures. ATC 24, Redwood City, USA: ATC

[16] Lumpkin EJ (2009): Enhanced seismic performance of multi-storey special concentrically brace frames using a balanced design procedure. *M.S. Thesis*, University of Washington.

